

Effect of Compaction and Preforming Parameters on the Compaction Behavior of Bonded Textile Preforms for Automated Composite Manufacturing

Wangqing Wu · Binyan Jiang · Lei Xie ·
Florian Klunker · Santiago Aranda · Gerhard Ziegmann

Received: 14 September 2012 / Accepted: 27 November 2012 / Published online: 24 January 2013
© Springer Science+Business Media Dordrecht 2013

Abstract The effect of compaction and preforming parameters on the Fiber Volume Fraction (FVF) and the Residual Preform Thickness (RPT) of bonded textile preforms during a compaction experiment was investigated by using Taguchi method. Four compaction and preforming parameters of compaction temperature (A), binder activation temperature (B), binder content (C) and binder activation time (D) were selected and optimized with respect to the FVF at specified compaction pressure (0.2 MPa) and the RPT after compaction. The results reveal that the compaction behavior of bonded textile preforms has been significantly influenced due to the presence of preforming binder. From all the selected experiment parameters the compaction temperature is the most influential factors on the FVF and RPT. The significant sequence of the parameters for the resulting FVF can be concluded as ABDC, which represents compaction temperature, binder activation temperature, binder activation time and binder content respectively, while this sequence is changed as ADCB as far as the RPT is concerned. The FVF during compaction and RPT during release were correlated with the compaction and preforming parameters using a modified four-parameter-compaction-model which has been proposed for describing the compaction behavior of bonded textile preforms.

Keywords A. Compaction behavior · B. Taguchi method · C. Bonded textile preforms · E. Composites manufacturing

W. Wu (✉) · F. Klunker · S. Aranda · G. Ziegmann
Institute of Polymer Materials and Plastic Engineering, Clausthal University of Technology,
Clausthal-Zellerfeld, Germany
e-mail: wangqing.wu@tu-clausthal.de

F. Klunker
Institute of Mechanical Systems, ETH Zurich, Zurich, Switzerland

W. Wu · B. Jiang
Department of Aeronautics and Astronautics, Central South University, Changsha, China

L. Xie
ABB Schweiz AG, RD-E2, Baden-Daettwil, Aargau, Switzerland

1 Introduction

For composites manufacturing processes, in particular Liquid Composites Molding (LCM) like Resin Transfer Molding (RTM) and Vacuum Assisted Resin Infusion (VARI), it is of great importance to understand the compaction behavior which describes the response of textile reinforcement under normal loading conditions. Because the compaction response of the textile reinforcement can affect both the manufacturing parameters like permeability and the mechanical properties of the final product due to the variation of Fiber Volume Fraction (FVF). In a typical RTM process a representation of the reinforcement stress profile, which can be obtained during a compaction experiment, is required in order to predict the distribution of forces applied to the RTM mold and thus to optimize the dimensioning of the tooling. Additionally, the Residual Preform Thickness (RPT), which is the difference between the initial preforms thickness and the permanent deformation after compaction, is also interested. This is because net shape preforms, which have nearly the same thickness as the impregnated parts, are essentially required in the cases where the cavity height can only be fixed so as to avoid complex mold design. In resin infusion processes like VARI, the permeability of the textile reinforcement is changing with the deformation of the textile reinforcement due to the use of flexible tooling. The impregnation of the textile reinforcement is then influenced by the variable permeability as a result of the variation of the FVF, which can be expressed as a function of the compaction pressure.

Many studies have been conducted on the compaction of textile reinforcement under various conditions [1–6]. In order to assess the influence of the temperature on the compaction behavior of textile reinforcement, Aranda et al. [1] applied different pre-heating conditions to preforms made of textile reinforcement layers with thermoplastic toughening fleece as interlayer in between. It has been observed that the thermoplastic toughening fleece undergoes a geometry change after heat treatment, leading to a contractive and wavy preform with increased initial preform thickness and therefore lower FVF. Interested by the influence of infiltration state on the compaction behavior of textile preforms, Hammami et al. [2] and Kelly et al. [3] studied the compaction behavior of different kinds of fabric preforms under dry and wet conditions. The compression and relaxation characteristics were found to depend on the structure of the textile preforms and the infiltration conditions as well. Similar investigations were also performed by Robitaille et al. [4–6] with dry and H₂O-saturated textile preforms made of woven fabrics. The compaction cycle number and the compaction rate respectively were confirmed to have the most pronounced effects on the compaction and relaxation behavior of the textile reinforcement. In addition, the compaction behavior of different textile reinforcements was investigated in [7–12], in which the mechanical behavior of textile preforms under normal load and the effect of diverse processing parameters on that behavior were extensively studied.

To identify the relationship between FVF and compaction pressure, a two parameter power law model was usually used to fit the experimental data [4]. During the investigation on a new sandwich textile reinforcement preforms developed for LCM processes, Luo et al. [13] used the two parameters power law model and a dissipated energy method to model the compaction and relaxation behavior respectively. It was found that when evaluating the compressibility of the multi-mat, mat, and woven fabrics, it is necessary to take the relaxation into account. The fabric relaxation behavior can be understood in terms of volumetric dissipation energy and fabric stiffness. In order to create a model for inclusion in flow simulations of LCM processes, Kelly et al. [3] and Bickerton et al. [14] investigated the viscoelastic compaction behavior of textile preforms. The studied textile preforms have displayed complex time-dependent response, including loading hysteresis, stress relaxation, and strain rate dependent loading behavior under no resin conditions. The significant influence of preform viscoelasticity was demonstrated by mold filling experiments [3].

And the viscoelastic response and the difference in behavior between the dry and wet samples observed were incorporated into a model of textile reinforcement deformation in [14]. The sample model is then used for both compaction and relaxation phases, and matches well experimental data over a range of FVFs and compression speeds. Furthermore, a three parameter power law model applied in [15, 16] for modeling the compaction behavior of textile reinforced reinforcement in VARI process (compaction pressure lower than 0.1 MPa) was found to be better than the two parameter power law model used in [4, 13].

Recently, in order to improve the process efficiency and preforms handling stability, bindered textile preform containing thermoset or thermoplastic binders between fabric layers was developed. At room temperatures the binders are usually in a solid state with powder or granulate form, which will melt at the so called activation temperatures so that the textile plies can be bonded together after a preforming cycle. In this way, the bindered textile preform can be transported or handled without damaging its textile structure such as fiber orientations. As a typical example, Greb et al. [17] developed an automated preforming center based on this concept. Considering the effect of the thermoplastic toughening fleece on the compaction behavior of the textile preform presented in [1], the compaction behavior of bindered textile preforms could also be affected because of the introduced preforming binder. Therefore, as an initial trial, Aranda et al. [18] studied the influence of preforming binder on the compaction behavior of textile preforms. The effects of binder type and binder content at higher temperatures on FVF, deformation and compaction pressure were analyzed.

Besides the compaction parameters such as compaction temperature, a number of process variables like binder activation temperature, binder activation time and binder content, are involved during the preforming stage, leading to a more complex compaction behavior of bindered textile preforms. Therefore, the purpose of this work is to investigate the effect of various compaction and preforming parameters on the interested performances such as FVF and RPT. Taguchi [19] parameter design method was applied for planning the experiment in order to save the experimental effort. Experimental data during the compaction and release process were analyzed and modeled for correlation between the compaction and preforming parameters and the FVF and RPT. The analysis of signal-to-noise (S/N) ratio and variance (ANOVA) were performed to specify the relevance of compaction and preforming parameters according to their importance on the FVF and the residual preforms thickness.

2 Experimental Procedure

2.1 Materials

2.1.1 Textile Reinforcement

Tri-axial glass fiber Non Crimp Fabric (NCF), provided by Institute of Textile Technology, RWTH Aachen, was used as the reinforcement material in the present research. The fiber orientations, glass roving and areal weight information are illustrated in Fig. 1. The preform configuration was according to the symmetric stacking sequence of [+45/−45/90]_s.

2.1.2 Binder

Epoxy powder binder EPIKOTE® Resin 05390 from HEXION special chemicals with melting point of 90 ± 15 °C, average particle size of 68.89 μm and epoxy equivalent of 905.5 ± 94.5 g/eq, is applied between two layers of reinforcements.

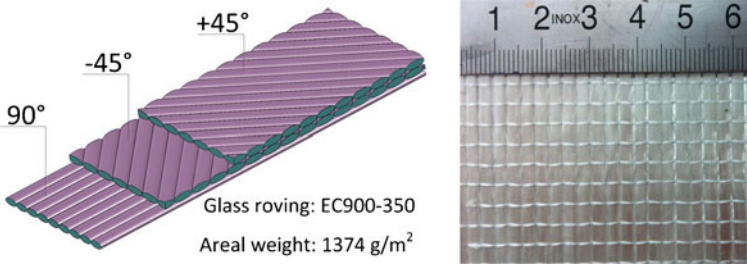


Fig. 1 Textile reinforcement

2.2 Specimen Preparation

A lab based binding process as shown in Fig. 2 was developed to prepare bindered textile preforms. With the help of an analysis (ISO 3310-1, 100 μm) sieve the required amount of binder was uniformly applied on the surface of the reinforcement. The amount of the binder is calculated as weight percentage referring to the weight of a single fabric layer. After applying binder, the other layer of reinforcement was put on the first layer with binder in between. Then the preform was laid carefully in a heated plate mold which was placed between two heated press plates to activate the applied binder with an activation temperature of 90 °C.

The preforms were cut into compaction test sample with 70 mm X 70 mm after activation of the binder. A schematic description of the compaction equipment is shown in Fig. 3. The samples were tested under controlled temperature conditions. The compaction area was defined by the size of the steel plated (50 mm X 50 mm) under the preforms. A preload of 400 Pa was used for the compaction experiment. The whole compaction process was divided into three stages which are compaction, holding deformation and release based on position control as shown in Fig. 4. The

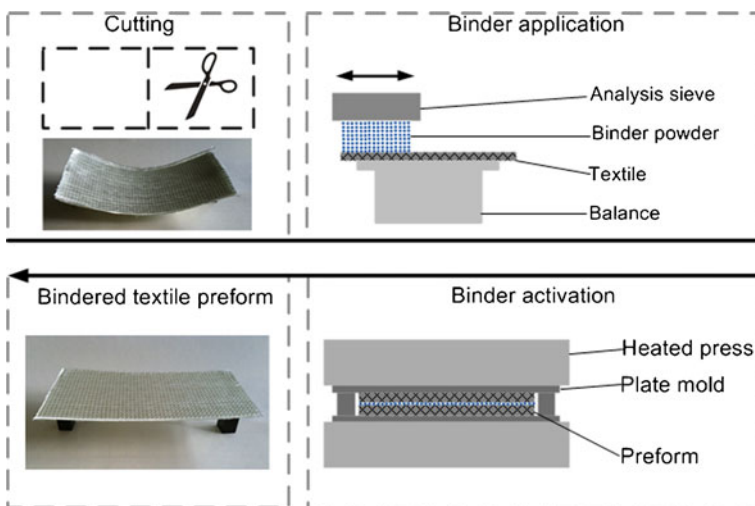


Fig. 2 Lab based binding process

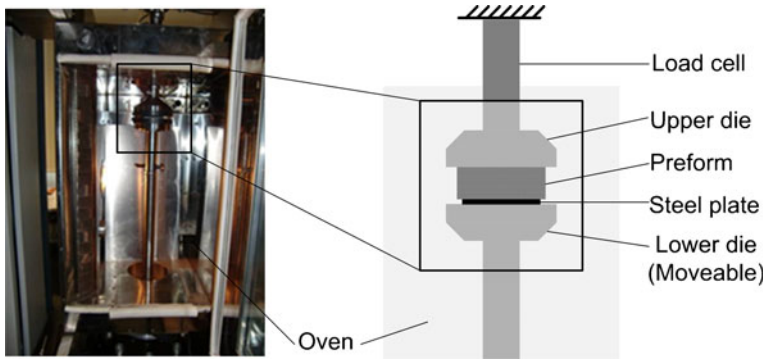


Fig. 3 Compaction experiment

FVF is calculated from the thickness data recorded during compaction experiment with the formula:

$$V_f = \frac{nA_f}{\rho h} \tag{1}$$

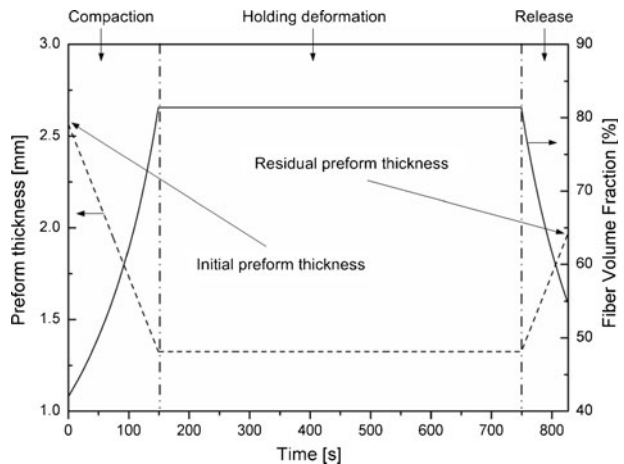
Where n is the number of fabric layers, A_f is the fabric areal density, ρ is the fiber density which is 2.55 g/cm^3 and h is the preform thickness. The RPT is the last data point recorded from the compaction experiment.

2.3 Design of Experiments

2.3.1 Taguchi Method

Generally, a lot of experiments have to be carried out when the number of parameters increase [20, 21]. And the traditional experimental design methods are too complex and difficult to use. In this context, Taguchi’s experimental design method was adopted in this

Fig. 4 Typical compaction procedure



study to provide a simple, efficient and systematic approach for optimization of experimental design for performance quality and cost [22, 23]. In the theory of Taguchi, the deviations between the experimental value and the desired value can be calculated by a loss function, which can be further transferred into a signal-to-noise (S/N) ratio, η . Depending on the type of characteristics, there are usually three S/N ratios available: the smaller the better (SB), the higher the better (HB), and the nominal the better (NB). The S/N ratios for each type of characteristic can be calculated as follows [24]:

Nominal is the best:

$$S/N_{NB} = 10 \log \left(\frac{\bar{y}}{S_y^2} \right) \quad (2)$$

Larger is the better (maximize):

$$S/N_{HB} = -10 \log \left(\frac{1}{n} \sum_{i=1}^n \frac{1}{y_i^2} \right) \quad (3)$$

Smaller is the better (minimize):

$$S/N_{SB} = -10 \log \left(\frac{1}{n} \sum_{i=1}^n y_i^2 \right) \quad (4)$$

Where \bar{y} is the average of the observed data, S_y^2 is the variance of y , n is the number of observations, and y is the observed data. Regardless of the category of the performance characteristics, the greater S/N ratio corresponds to the better performance. Therefore, the optimal level of the process parameters is the highest S/N ratio.

In compaction of textile preforms, higher FVF at specified compaction pressure and lower RPT after a compaction cycle are indications of better performance. Therefore, the “HB” and “LB” ratios were selected respectively for FVF and RPT to obtain optimum compaction performance.

2.3.2 Experiment Design

Table 1 indicates the compaction and preforming parameters (factors) and their values (levers). The factors chosen for the compaction experiments were: (1) compaction temperature, T_{comp} , (2) binder activation temperature, T_{act} , (3) binder content, c and (3) binder activation time, t . Each parameter has four levels, denoted 1, 2, 3 and 4. Worth to mention is, a wider range of compaction temperatures starting from 25 °C up to 190 °C were considered

Table 1 Compaction and preforming parameters used in the experiments

Levels	Factors			
	Compaction temperature A [°C]	Binder activation temperature B [°C]	Binder content C [wt.%]	Binder activation time D [min]
1	25	90	1	0.5
2	60	100	3	1.0
3	125	110	5	1.5
4	190	120	7	2.0

for the corresponded four different material states of the binder including solid (25 °C), partly melted (60 °C), fully melted higher viscous (125 °C) and fully melted lower viscous (190 °C). The compaction behavior of bindered textile preforms was studied under the four material states of binder which can be further corresponded to different applications such as the highest level of 190 °C is interested for LCM processes with thermoplastic resin [25].

To save the experimental effort, orthogonal arrays, in which the columns for the independent variables are orthogonal to one another, are often employed in industrial experiments to study the effect of several control factors. In this study, an L_{16} orthogonal array with four columns and 16 rows was used as shown in Table 2, where the FVF results were taken when the compaction pressure increases up to 0.2 bar. And the RPT results were taken after the compaction cycle. Each experiment was conducted at least three times in order to ascertain the effect of material and test system variability. Since the influence of the interaction between the preforming parameters such as the activation temperature and the activation time on the results was not clear, a more complex interactive experimental design was not considered in the present study.

3 Results and Discussion

3.1 Fiber Volume Fraction (FVF)

3.1.1 Compaction and Preforming Parameters Effects Analysis

The experimental results for the FVF, corresponding standard deviation and S/N ratios are as shown in Table 2. The mean S/N ratio for each level of the parameters was calculated and

Table 2 Experimental design using the L_{16} orthogonal array and experimental results

Exp. no.	A [°C]	B [°C]	C [%]	D [min]	Evaluation					
					FVF (%)	Std. of FVC	S/N for FVC	RPT (mm)	Std. of RPT	S/N for RPT
1	1(25)	1 (90)	1 (1)	1 (0.5)	64.65	0.28	36.21	1.94	0.03	-5.75
2	1	2 (100)	2 (3)	2 (1.0)	64.35	0.33	36.17	1.93	0.01	-5.71
3	1	3 (110)	3 (5)	3 (1.5)	62.83	0.72	35.96	1.94	0.02	-5.75
4	1	4 (120)	4 (7)	4 (2.0)	61.75	0.43	35.81	1.99	0.02	-6.02
5	2 (60)	1	2	3	65.10	0.66	36.27	1.84	0.02	-5.31
6	2	2	1	4	63.30	0.89	36.03	1.93	0.04	-5.69
7	2	3	4	1	63.25	0.38	36.02	1.85	0.01	-5.33
8	2	4	3	2	63.61	0.34	36.07	1.85	0.01	-5.34
9	3 (125)	1	3	4	67.13	0.53	36.54	1.88	0.03	-5.49
10	3	2	4	3	66.78	0.36	36.49	1.87	0.02	-5.45
11	3	3	1	2	66.44	0.66	36.45	1.89	0.01	-5.54
12	3	4	2	1	67.74	0.15	36.62	1.85	0.01	-5.35
13	4 (190)	1	4	2	69.33	0.13	36.82	1.85	0.01	-5.32
14	4	2	3	1	69.56	0.59	36.85	1.81	0.01	-5.18
15	4	3	2	4	67.66	1.67	36.61	1.89	0.05	-5.53
16	4	4	1	3	68.85	1.12	36.76	1.87	0.04	-5.41

summarized in Table 3. Additionally, the total mean S/N ratio is computed by averaging the total mean S/N ratios. Based on the data presented in Table 3, the optimal compaction performance for FVF was obtained at 190 °C compaction temperature (Level 4), 90 °C binder activation temperature (Level 1), 3 % binder content (Level 2) and 0.5 min binder activation time (Level 1) settings. Figures 5 and 6 shows the comparison of the predicted and actual and residual and actual S/N ratios for the FVF using regression analysis. Most of the points are close to the line and the deviations are very small and negligible. With respect to the coefficient of multiple determinations (R^2) of the fitted model, also known as R^2 -statistics, the value of R^2 obtained for the FVF is 0.989. This means that the model as fitted explains 98.9 % of the variability of FVF.

The compaction temperature represents a positive effect on the FVF. The average value of S/N ratio of compaction temperature increases with increasing compaction temperature as shown in Table 3. This result means that higher FCF can be achieved with higher compaction temperature. The positive effect from the compaction temperature can be further confirmed in Fig. 7, where the relationship between FVF and compaction pressure was record under various compaction temperatures (Exp. No. 2, 5, 12, 15). As shown in Fig. 7, although there are meanwhile effects from preforming parameters (Binder activation temperature and binder activation time), the FVF indicates an obvious increase with increasing compaction temperature under the same compaction pressure. This can be attributed to the higher range of S/N ratio of compaction temperature (0.72), which is about 2.6–3.2 times higher than the range of the other two preforming parameters (Table 3). The higher range of S/N ratio from compaction temperature means more significant influence on the FVF so that the effects from the two preforming parameters cannot readily be shown up. It is believed that the effect of compaction temperature on the FVF can be related to the four material state of the binder. Because the four selected levels of compaction temperature correspond to the four material states of the binder, which is solid (level 1, 25 °C), partly melted (level 2, 60 °C), fully melted higher viscous (level 3, 125 °C) and fully melted lower viscous (level 4, 190 °C). The compressibility of the bindered textile preforms can be tailored by the compaction temperature due to the fact that the re-organization of the fibers can be facilitated by the lubricating effect from the melted preforming binder.

3.1.2 Correlation Between Compaction and Preforming Parameters and FVF

Several studies have been shown that the compaction response of fabrics can be expressed by a three parameter power law model representing the FVF as a function of the compaction pressure [15, 16]:

$$V_f = a \cdot P^b + c \tag{5}$$

Table 3 Response table mean signal-to-noise (S/N) ratio for FVF factor and significant interaction

Symbol	Processing parameters	Average value of S/N				
		Level 1	Level 2	Level 3	Level 4	Range (max-min)
A	Compaction temperature	36.04	36.10	36.52	36.76 ^a	0.72
B	Binder activation temperature	36.46 ^a	36.38	36.26	36.32	0.20
C	Binder content	36.36	36.42 ^a	36.36	36.29	0.13
D	Binder activation time	36.42 ^a	36.38	36.37	36.25	0.17

Total mean S/N ratio = 36.35; ^a Optimum level

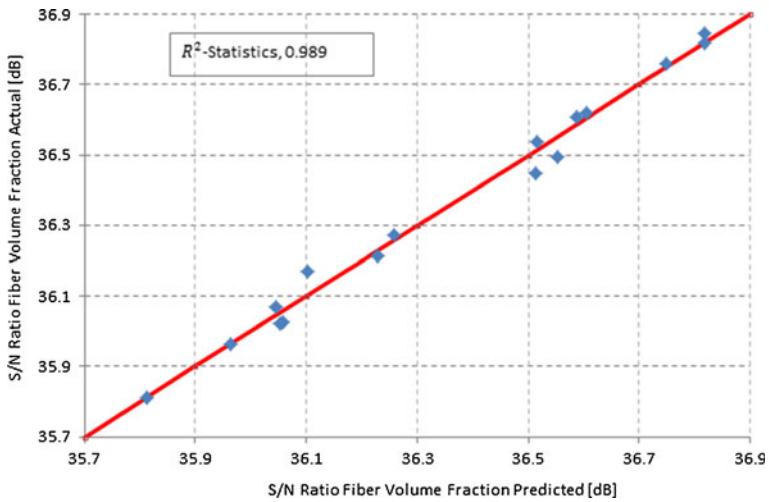


Fig. 5 Comparison of actual and predicted S/N ratios of FVF using linear regression analysis

where V_f is FVF, P is the compaction pressure and c is referred to the initial FVF under 0 MPa compaction pressure.

As for the non-crimped fabrics preforms with or without binder used in this study, this three parameters model can only express the compaction response in a limited range (<0.1 MPa) as shown in Fig. 8. To approximate the FVF with more accuracy, an improved model must be developed for bindered textile preforms. Therefore, the authors propose a modified four parameters model by multiplying formula 5 and an exponential function as:

$$V_f = (a \cdot P^b + c) e^{d \cdot P} \tag{6}$$

where V_f and P have the same meaning as Eq. 4, and a , b , c , and d are constants, e is the number such that the function e^x is its own derivation. The fitting results with

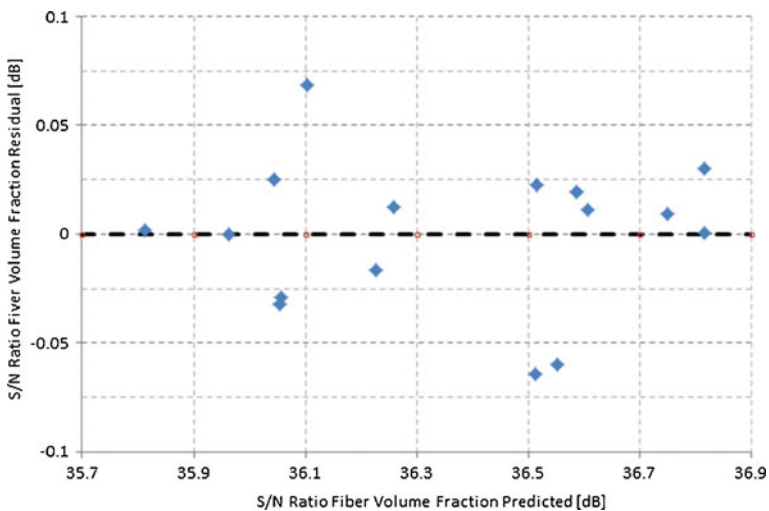


Fig. 6 Comparison of residual and predicted S/N ratios of FVF using linear regression analysis

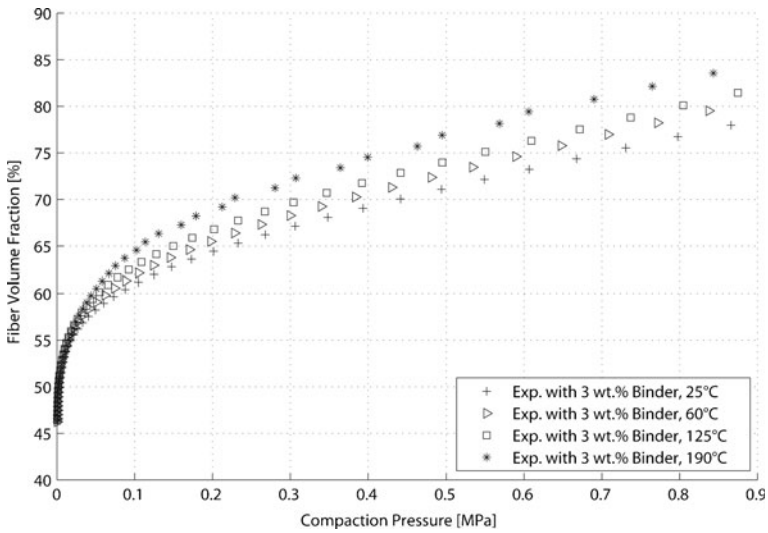


Fig. 7 Effect of compaction temperature on the FVF

modified four parameter model are as shown in Fig. 9. As we can see the modified four parameters model can make a better prediction of compaction response of bindered textile preforms. To show the modeling ability of the proposed model in higher compaction temperatures, further attempts to fit the experiments data with 60 °C, 125 °C and 190 °C were performed. Again good agreement between the experimental data and the fitted results is as shown in Fig. 10. Therefore, this model will be adopted to correlate the FVF and the compaction and preforming parameters as shown in Table 1.

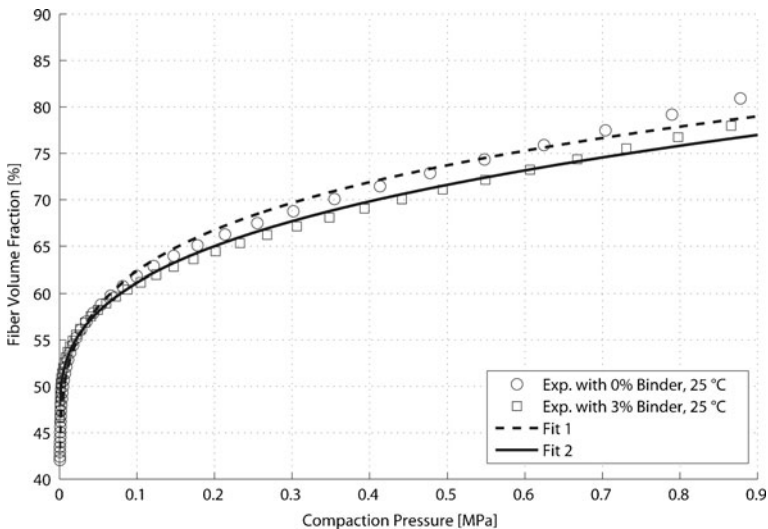


Fig. 8 Fitting of compaction curve of textile preforms with three parameters power law model

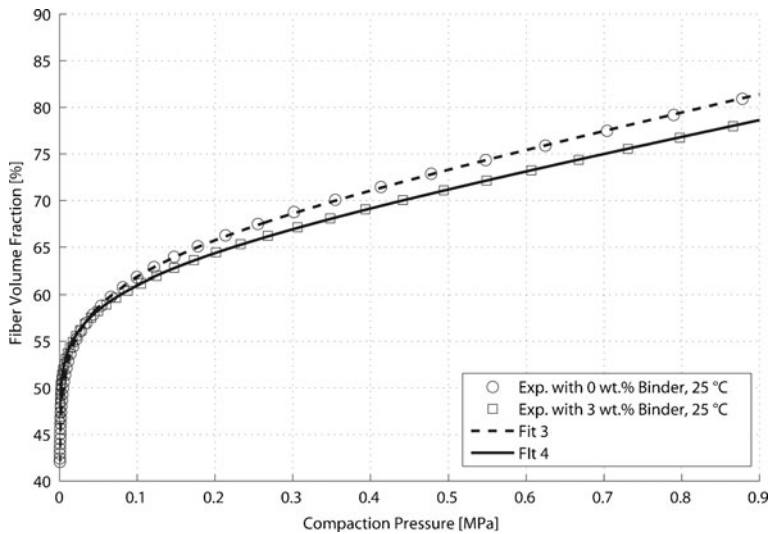


Fig. 9 Fitting of compaction curve of bindered textile preforms with proposed model

The equation of the model proposed for correlation between the FVF and the compaction and preforming parameters is according to Eq. 6 by correlating its four parameters with compaction temperature, binder activation temperature, binder content and binder activation time using linear regression as shown in Eq. 7. The FVF at specified compaction pressure can be estimated by Eq. 6 with the four parameters calculated with Eq. 7 and the compaction pressure equals to 0.2 MPa in the present study.

$$\begin{bmatrix} a \\ b \\ c \\ d \end{bmatrix} = \begin{bmatrix} 259.43 & 0.627 & -105.278 & -0.153 \\ -0.915 & -9.21E-03 & 0.211 & 5.43E-03 \\ -2.236 & -3.74E-03 & 1.468 & 2.45E-03 \\ -4886.541 & 14.158 & 3980.552 & -10.819 \\ -49.439 & -0.708 & 8.292 & 0.364 \\ 0.01 & 7.83E-05 & -3.31E-03 & -4.87E-05 \\ 22.059 & -0.045 & -16.801 & 0.016 \\ 0.051 & 0.006 & 0.172 & -4.39E-03 \\ 48.971 & -0.174 & -43.192 & 0.121 \\ 0.414 & 0.007 & -0.018 & -3.48E-03 \\ 1161.298 & -2.318 & -794.078 & 5.762 \\ -0.235 & 8.88E-04 & 0.209 & -3.79E-04 \\ -1E-04 & -6.39E-05 & -2.234E-03 & 4.279E-05 \\ -11.396 & 0.023 & 8.47 & -0.055 \end{bmatrix}^T \begin{bmatrix} 1 \\ T_{comp} \\ T_{act} \\ c \\ t \\ T_{comp} \times T_{act} \\ T_{comp} \times c \\ T_{comp} \times t \\ T_{act} \times c \\ T_{act} \times t \\ c \times t \\ T_{comp} \times T_{act} \times c \\ T_{comp} \times T_{act} \times t \\ T_{act} \times c \times t \end{bmatrix} \quad (7)$$

3.2 Residual Preform Thickness (RPT)

3.2.1 Compaction and Preforming Parameters Effects Analysis

The experimental results for the RPT, corresponding standard deviation and S/N ratios are also as shown in Table 2. The mean S/N ratio for each level of the parameters

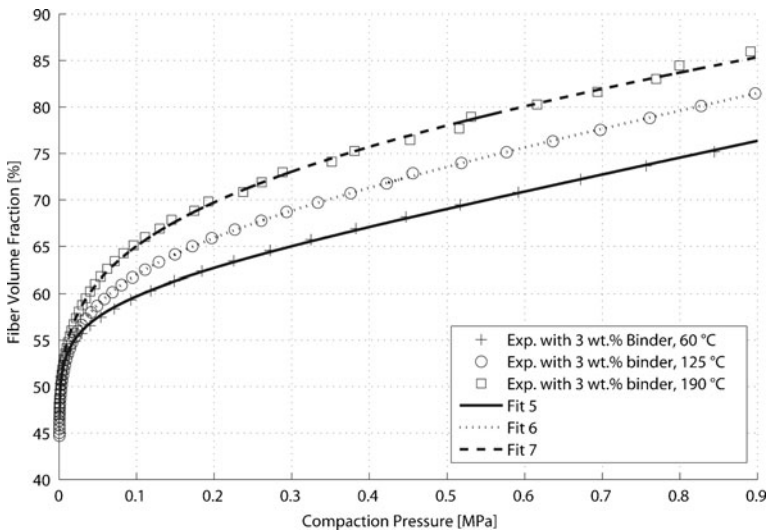


Fig. 10 Fitting of compaction curve of bindered textile preforms with proposed model

was calculated and summarized in Table 4. Additionally, the total mean S/N ratio is computed by averaging the total mean S/N ratios. Based on the data presented in Table 4, the optimal compaction performance for RPT was obtained at 190 °C compaction temperature (Level 4), 90 °C binder activation temperature (Level 1), 5 % binder content (Level 3) and 0.5 min binder activation time (Level 1) settings. In Figs. 11 and 12 the actual and predicted S/N ratios and residual and predicted S/N ratios for RPT were compared using linear regression analysis. Here, R^2 of the model is 0.999.

As the FVF, the performance of higher mold temperature is positive for RPT as well as shown in Table 4. The range of S/N ratio of compaction temperature again results a maximum of 0.45, indicating that the compaction temperature has the most significant influence on the RPT. Figure 13 shows the effect of the compaction temperature and the binder content on the RPT after a compaction cycle. It is

Table 4 Response table mean signal-to-noise (S/N) ratio for RPT factor and significant interaction

Symbol	Processing parameters	Average value of S/N				
		Level 1	Level 2	Level 3	Level 4	Range (max-min)
A	Compaction temperature	-5.81	-5.42	-5.46	-5.36 ^a	0.45
B	Binder activation temperatur	-5.47 ^a	-5.51	-5.54	-5.53	0.07
C	Binder content	-5.60	-5.47	-5.44 ^a	-5.53	0.16
D	Binder activation time	-5.40 ^a	-5.48	-5.48	-5.68	0.28

Total mean S/N ratio = -5.51; ^a Optimum level

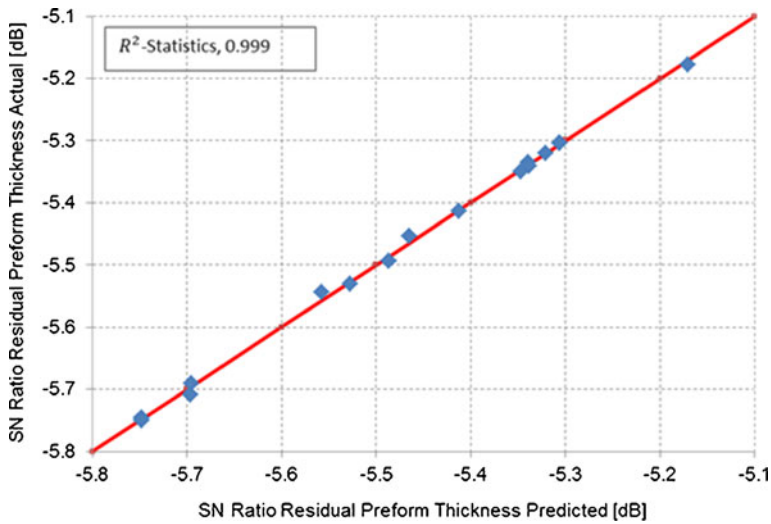


Fig. 11 Comparison of actual and predicted S/N ratios of RPT using linear regression analysis

obvious to see that the RPT was influenced by the compaction temperature and this influence is further strengthened for the bindered textile preforms. For each compaction temperature, the RPT of the bindered textile preform is smaller than the one without binder. This may be attributed to the limited relaxation because of the bindered fiber bundles. Starting with a lower compaction temperature of 25 °C, the RPT of bindered textile preform undergoes first a decrement when the compaction temperature increases up to 60 °C. This phenomenon can be explained that the partly melted interlayer of binder are compressed into the fiber bundles of both upper and lower fabric layer and act as binder so that the relaxation of fiber bundles

Fig. 12 Comparison of residual and predicted S/N ratios of RPT using linear regression analysis

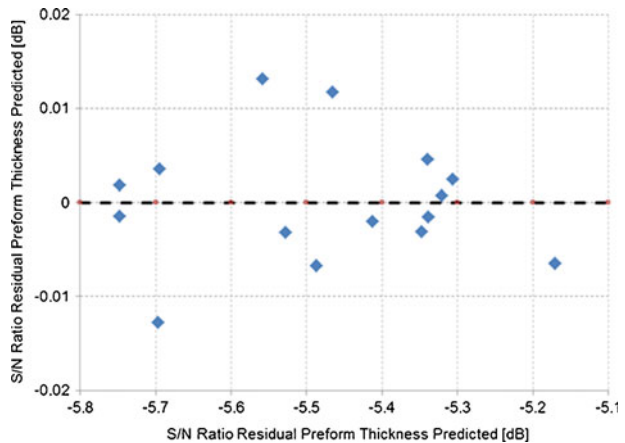
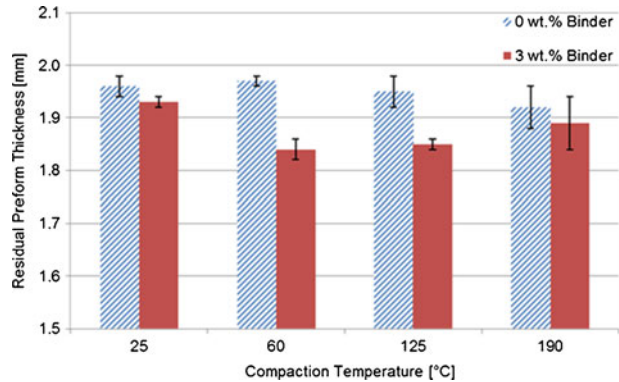


Fig. 13 Effect of compaction temperature and binder content on the RPT



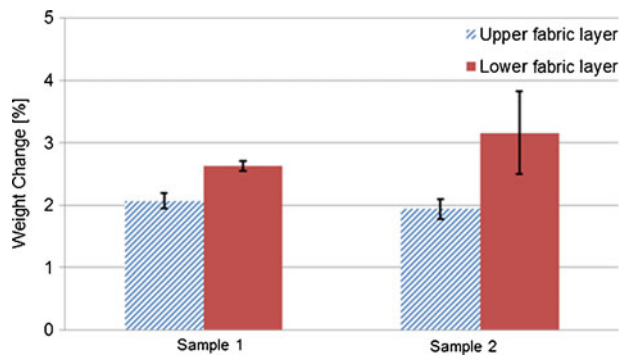
is greatly limited. However, at higher compaction temperatures where the binder is fully melted, instead of decrement the RPT compressed at 125 °C shows a slight increment which becomes more remarkable at 190 °C. It is believed that the increment of RPT may be attributed to the inertial effect of the binder melt with lower viscosity. Large amounts of binder melt flow into the lower fabric layer, leading to a less bindered upper fabric layer with larger relaxation because of the released fiber bundles. As shown in Fig. 14 the weight change of lower fabric layer is obviously higher than the upper fabric layer when both of them were placed in the oven with 500 °C for 1 h, which further shows that there are more residual binder in lower fabric layer.

3.2.2 Correlation Between Compaction and Preforming Parameters and RPT

During the release process the correlation between the preform thickness and the compaction pressure can be derived from Eq. 1:

$$h = \frac{A_f \times n}{V_f \times p} \tag{8}$$

Fig. 14 Weight Change of both fabric layers after compression at 190 °C and burn down at 500 °C



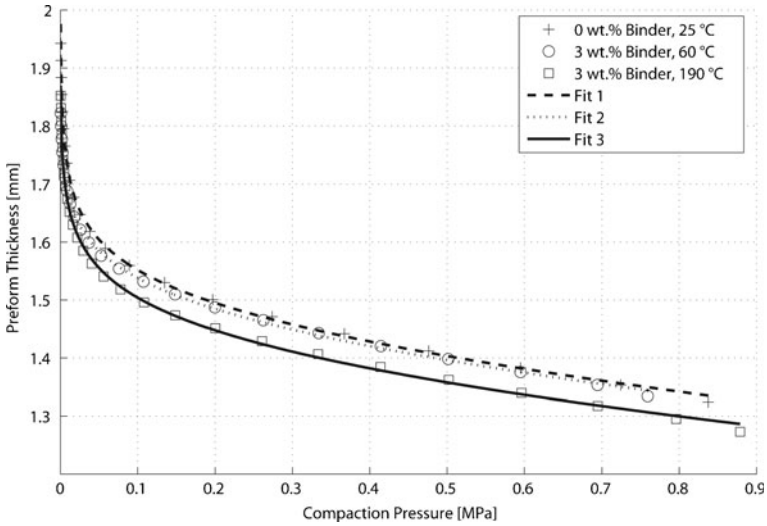


Fig. 15 Fitting of release curve of bindered textile preforms

Substituting Eq. 6 into Eq. 7 with consideration of the density of glass fibers and the preform configuration, the preform thickness h as a function of the compaction pressure P during the release process is:

$$h = \frac{1.0776}{(a \cdot P^b + c)e^{d \cdot P}} \tag{9}$$

where a , b , c , d and e have the same meaning as Eq. 6. The RPT is obtained when the compaction pressure equals to the preload. Fitting trials with Eq. 9 to the release curves of compaction experiment are as shown in Fig. 15. The fitted results show good agreement with the experimental results. The RPT from the experiment and calculated with Eq. 9 are compared in Fig. 16. These results confirm that the proposed model can make a good

Fig. 16 Comparison of the RPT from the experiment and the model

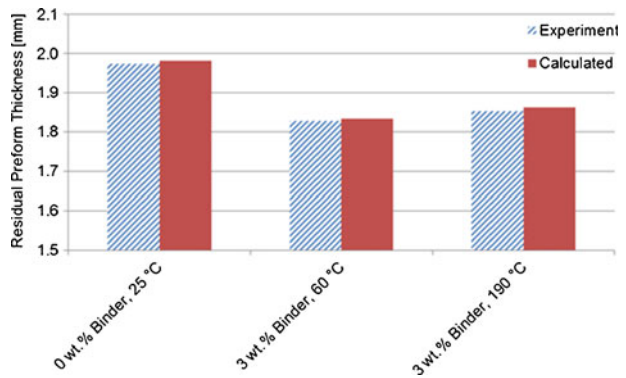


Table 5 Results of ANOVA for FVF

Parameters	Degree of freedom	Sum of square	Mean square	F ratio	Contribution (%)
Compaction temperature	3	82.02	27.34	690.34	88.17
Binder activation temperature	3	5.07	1.69	42.67	5.33
Binder content	3	1,77	0.59	14.88	1.77
Binder activation time	3	3.92	1.31	32.96	4.09
Error	3	0,12	0.04	–	–
Total	15	92.89	–	–	–

prediction of the RPT. Therefore, the model will be further applied to correlate the RPT and the process variables.

The equation of the model proposed for the RPT is according to Eq. 8 by correlating its four parameters with compaction temperature, binder activation temperature, binder content and binder activation time as shown in Eq. 10. The RPT after a compaction cycle can be estimated by Eq. 8 with the four parameters calculated by Eq. 10 and the compaction pressure equals to the pre-load.

$$\begin{bmatrix} a \\ b \\ c \\ d \end{bmatrix} = \begin{bmatrix} 0 & 0 & 0 & 0 \\ 6.59E-05 & 0.0034 & 0.0077 & -0.0008 \\ 0.0045 & 0.0009 & 0.0035 & -0.0007 \\ 58.7168 & -28.2973 & -68.7473 & 6.5201 \\ -1.0823 & 0.6539 & 2.12 & -0.0326 \\ 3.75E-063 & -3.39E-05 & -7.58E-05 & 8.23E-06 \\ -0.2995 & 0.1327 & 0.3606 & -0.01777 \\ 0.0109 & -0.0071 & -0.0199 & 0.0011 \\ -0.5817 & 0.2638 & 0.6519 & -0.0581 \\ 0.0093 & -0.0061 & -0.0199 & 0.0003 \\ -11.3092 & 6.2629 & 10.7919 & -1.9508 \\ 0.0028 & -0.0012 & 0.0034 & 0.0001 \\ -0.0001 & 6.63E-05 & 0.0002 & -1.02E-05 \\ 0.1204 & -0.0574 & -0.0978 & 0.018 \end{bmatrix}^T \begin{bmatrix} 1 \\ T_{comp} \\ T_{act} \\ c \\ t \\ T_{comp} \times T_{act} \\ T_{comp} \times c \\ T_{comp} \times t \\ T_{act} \times c \\ T_{act} \times t \\ c \times t \\ T_{comp} \times T_{act} \times c \\ T_{comp} \times T_{act} \times t \\ T_{act} \times c \times t \end{bmatrix} \tag{10}$$

Table 6 Results of ANOVA for RPT

Parameters	Degree of freedom	Sum of square	Mean square	F ratio	Contribution (%)
Compaction temperature	3	0.0233	0.0078	134.59	65.67
Binder activation temperature	3	0.0006	0.0002	3.68	1.32
Binder content	3	0.0027	0.0009	15.88	7.32
Binder activation time	3	0.0084	0.0028	48.28	23.24
Error	3	0.0002	0.00006	–	–
Total	15	0.0352	–	–	–

Table 7 Results of the confirmation experiment for FVF

	Initial experimental parameters	Optimal experimental parameters	
		Predicted	Experiment
Level	A1B2C1D1	A4B1C2D1	A4B1C2D1
FVC (%)	64.88	–	67.95
S/N ratio (dB)	36.24	36.72	36.64
Improvement of S/N ratio	–	0.40	–

3.3 Significant Sequence Analysis

The statistical analysis of variance (ANOVA) was conducted to determine more accurately the optimum combination of the experiment parameters and to specify the relative importance of the design parameters on the FVF and RPT. The analysis is carried out for the level of significance of 1 % (the level of confidence is 99 %) [26, 27]. Tables 5 and 6 show the results of the ANOVA analysis for the experiment output, respectively. The last columns of Tables 5 and 6 indicate the percentage contribution of each factor on the total variation, indicating their degree of influence on the results. The greater the percentage contribution, the greater the influence a factor has on the performance. According to Table 5, the compaction temperature was found to be the major factor affecting the FVF (88.17 %), whereas the binder activation temperature, binder content and binder activation time affect the FVF by 5.33 %, 1.77 % and 4.09 %, respectively. The change of preforming parameters in the range given in Table 1 has an insignificant effect on the FVF. Table 6 shows the results of the ANOVA for RPT, it can be found that the compaction temperature again is the most significant design parameter for affecting RPT (65.67 %). The binder activation time affects the RPT by 23.24 %. The binder activation temperature and binder content has an insignificant effect on the RPT (1.32 % and 7.32 %, respectively).

3.4 Verification Experiments

To validate the conclusions drawn during the analysis phase verification experiments were performed to predict and verify the improvement of the performance characteristics using the

Table 8 Results of the confirmation experiment for RPT

	Initial experimental parameters	Optimal experimental parameters	
		Predicted	Experiment
Level	A1B2C1D1	A4B1C3D1	A4B1C3D1
RPT (mm)	1.93	–	1.86
S/N ratio (dB)	–5.71	–4.94	–5.39
Improvement of S/N ratio	–	0.32	–

optimal level of the experiment parameters. The predicted S/N ratio $\hat{\eta}$ using the results of regression analysis can be calculated with Eq. 11.

$$\begin{bmatrix} \hat{\eta}_{FVC} \\ \hat{\eta}_{RPT} \end{bmatrix} = \begin{bmatrix} 6.47 & -10.789 \\ -0.006 & 0.062 \\ -0.002 & 0.052 \\ 14.284 & -168.588 \\ 0.108 & 9.052 \\ 0.0001 & -0.0006 \\ 0.0195 & 0.675 \\ -0.0008 & -0.076 \\ -0.205 & 1.527 \\ -0.003 & -0.091 \\ 4.861 & 30.117 \\ 0 & 0.0065 \\ 0 & 0.0007 \\ 0 & -0.194 \end{bmatrix}^T \begin{bmatrix} 1 \\ T_{comp} \\ T_{act} \\ c \\ t \\ T_{comp} \times T_{act} \\ T_{comp} \times c \\ T_{comp} \times t \\ T_{act} \times c \\ T_{act} \times t \\ c \times t \\ T_{comp} \times T_{act} \times c \\ T_{comp} \times T_{act} \times t \\ T_{act} \times c \times t \end{bmatrix} \tag{11}$$

Table 7 shows the results of the confirmation experiments using the optimal experimental parameters for FVF. The increase of S/N ratio from the initial experimental parameters to the level of optimal experimental parameters is 0.40 dB. The FVF is improved by 4.7 %. Table 8 shows the results of the confirmation experiments using the optimal experimental parameters for RPT. The increase of S/N ratio from the initial experimental parameters to the level of optimal experimental parameters is 0.32 dB. The RPT is reduced by 3.6 %. Good agreement between the predicted experimental performance and actual experimental performance was observed. The FVF and RPT are both improved by using the approach.

The experimental results confirmed the validity of the applied Taguchi method for enhancing the experimental performance and optimizing compaction and preforming parameters. However, the FVF (67.95 %) with optimal experimental parameters is about 2.3 % lower than the value (69.56 %) from experiment number 14 and the difference for residual preforms thickness is 2.7 % (1.86 mm vs. 1.81 mm). It is believed that the concluded optimal experiment parameters combination in this research is not really optimal with the current experimental plan. Because the interactions among the experiment parameters like the binder activation temperature and binder activation time were not considered in the current study, which may also have an influence the analyzed optimal result. Moreover, there are a great number of steps in the serious experiments starting from the bindered preforms preparation to the compaction experiment. There could be in each of the steps a human error source that could have an influence on the final results. Therefore, it is necessary to consider the parameter interaction and the accumulating human error effect for further research to acquire a better optimal experiment parameter combination.

4 Conclusion

In this study, an investigation on the effect of the compaction and preforming parameters on the FVF and RPT based on the Taguchi method has been performed and presented.

Summarizing the mean experimental results of this study, the following generalized conclusions can be drawn:

- (1) Based on the signal-to-noise ratio results, the optimal compaction and preforming parameters settings for FVF and RPT are compaction temperature 190 °C, binder activation temperature 90 °C, binder content, 3 %, binder activation time 0.5 min and compaction temperature 190 °C, binder activation temperature 90 °C, binder content 5 %, binder activation time 0.5 min, respectively.
- (2) The compaction behavior of bindered textile preforms has been significantly influenced due to the presence of binder. Instead of the commonly applied three parameter model that correlates the FVF and the compaction pressure during compaction of textile preforms under 0.1 MPa, a modified four parameter model was proposed to extend the modeling range up to 0.9 MPa. The fitted results have shown that the proposed modified four parameter model can make more accurate prediction of compaction and release response of the bindered textile preforms. Based on the proposed model the FVF and RPT can be correlated well with the compaction and preforming parameters with the help of linear regression method.
- (3) Based on the analysis of variance results, the highly effective parameters on both the FVF and RPT were determined. Namely, the compaction temperature is the main factor that has the highest importance on the FVF. The preforming parameters, that are, binder activation temperature, binder content and binder activation time does not seem to have much of an influence on the FVF. The RPT is affected strongly by the compaction temperature (65.67 %), whereas the binder activation time, binder content and binder activation temperature have a significant statistical influence.
- (4) The improvement of the FVF from the initial compaction and preforming parameters to the optimal compaction and preforming parameters is about 4.7 %, whereas the RPT is improved by 3.6 %. The regression results showed that the deviations between the actual and predicted S/N ratios of both FVF and RPT are small for each parameter.
- (5) The optimal experiment parameter combinations for both FVF and RPT do not lead to optimal results due to the interaction among the factors. Taguchi method with interactive parameter design and accumulated human error should be considered for further research to acquire a more accurate optimal experiment parameter combination.

Acknowledgments The authors wish to acknowledge the financial support from Forschungskuratorium textile (FKT) and Chinese Scholarship Council (CSC). A word of thanks also goes to the Institute of Textile Technology Aachen for supplying the textile reinforcement in the frame of scientific research project DFG-AiF-Cluster “Leichtbau und Textilien”. Additional thanks also go to Zhe Liu for conducting the series experiments.

References

1. Aranda, S., Klunker, F., Ziegmann, G.: Compaction response of fiber reinforcements depending on processing temperature. In: Proceedings of ICCM17, Edinburgh (2009)
2. Hammami, A.: Effect of reinforcement structure on compaction behavior in the vacuum infusion process. *Polym. Compos.* **22**(3), 337–348 (2001). doi:10.1002/pc.10542
3. Kelly, P.A., Umer, R., Bickerton, S.: Viscoelastic response of dry and wet fibrous materials during infusion processes. *Compos. A: Appl. Sci. Manuf.* **37**(6), 868–873 (2006). doi:10.1016/j.compositesa.2005.02.008
4. Robitaille, F., Gauvin, R.: Compaction of textile reinforcements for composites manufacturing. I: review of experimental results. *Polym. Compos.* **19**(2), 198–216 (1998). doi:10.1002/pc.10091

5. Robitaille, F., Gauvin, R.: Compaction of textile reinforcements for composites manufacturing. II: compaction and relaxation of dry and H₂O-saturated woven reinforcements. *Polym. Compos.* **19**(5), 543–557 (1998). doi:[10.1002/pc.10128](https://doi.org/10.1002/pc.10128)
6. Robitaille, F., Gauvin, R.: Compaction of textile reinforcements for composites manufacturing. III. Reorganization of the fiber network. *Polym. Compos.* **20**(1), 48–61 (1999). doi:[10.1002/pc.10334](https://doi.org/10.1002/pc.10334)
7. Batch, G.L., Cumiskey, S., Macosko, C.W.: Compaction of fiber reinforcements. *Polym. Compos.* **23**(3), 307–318 (2002). doi:[10.1002/pc.10433](https://doi.org/10.1002/pc.10433)
8. Chen, B.X., Chou, T.W.: Compaction of woven-fabric preforms in liquid composite molding processes: single-layer deformation. *Compos. Sci. Technol.* **59**(10), 1519–1526 (1999). doi:[10.1016/s0266-3538\(99\)00002-0](https://doi.org/10.1016/s0266-3538(99)00002-0)
9. Kim, Y.R., McCarthy, S.P., Fanucci, J.P.: Compressibility and relaxation of fiber reinforcements during composite processing. *Polym. Compos.* **12**(1), 13–19 (1991). doi:[10.1002/pc.750120104](https://doi.org/10.1002/pc.750120104)
10. Kruckenburg, T., Parton, R.: Compaction of dry and lubricated reinforcements. In: *Proceedings FPCM-7, Delaware* (2004)
11. Pearce, N., Summerscales, J.: The compressibility of a reinforcement fabric. *Compos. Manuf.* **6**(1), 15–21 (1995). doi:[10.1016/0956-7143\(95\)93709-s](https://doi.org/10.1016/0956-7143(95)93709-s)
12. Saunders, R.A., Lekakou, C., Bader, M.G.: Compression in the processing of polymer composites 1. A mechanical and microstructural study for different glass fabrics and resins. *Compos. Sci. Technol.* **59**(7), 983–993 (1999). doi:[10.1016/s0266-3538\(98\)00137-7](https://doi.org/10.1016/s0266-3538(98)00137-7)
13. Luo, Y.W., Verpoest, I.: Compressibility and relaxation of a new sandwich textile preform for liquid composite molding. *Polym. Compos.* **20**(2), 179–191 (1999). doi:[10.1002/pc.10345](https://doi.org/10.1002/pc.10345)
14. Bickerton, S., Buntain, M.J., Somashekar, A.A.: The viscoelastic compression behavior of liquid composite molding preforms. *Compos. A: Appl. Sci. Manuf.* **34**(5), 431–444 (2003). doi:[10.1016/s1359-835x\(03\)00088-5](https://doi.org/10.1016/s1359-835x(03)00088-5)
15. Klunker, F., Aranda, S., Ziegmann, G.: Permeability and compaction models for non-crimped fabrics to perform 3D simulations of vacuum assisted resin infusion. In: *The 9th International Conference on Flow Processes in Composite Materials*, Montreal, Canada (2008)
16. Yang, J.S., Xiao, J.Y., Zeng, J.C., Jiang, D.Z., Peng, C.Y.: Compaction behavior and part thickness variation in vacuum infusion molding process. *Appl. Compos. Mater.* **19**(3–4), 443–458 (2012). doi:[10.1007/s10443-011-9217-8](https://doi.org/10.1007/s10443-011-9217-8)
17. Greb, C., Schnabel, A., Linke, M.: New technology and process chains for high volume production of textile preforms. Paper presented at the 17th SAMPE Germany conference, Aachen
18. Aranda, S., Klunker, F., Ziegmann, G.: Influence of the binding system in the compaction behavior of NCF carbon fiber reinforcement. In: *Proceedings of ICCM18, Jeju* (2011)
19. Unal, R., Dean, E.B.: Taguchi approach to design optimization for quality and cost: an overview. In: *Proceedings of the 13th Annual Conference of the International Society of Parametric Analysis, Louisiana* (1991)
20. Lin, T.R.: Optimisation technique for face milling stainless steel with multiple performance characteristics. *Int. J. Adv. Manuf. Technol.* **19**(5), 330–335 (2002). doi:[10.1007/s001700200021](https://doi.org/10.1007/s001700200021)
21. Yang, W.H., Tarnag, Y.S.: Design optimization of cutting parameters for turning operations based on the Taguchi method. *J. Mater. Process. Technol.* **84**(1–3), 122–129 (1998). doi:[10.1016/s0924-0136\(98\)00079-x](https://doi.org/10.1016/s0924-0136(98)00079-x)
22. Shaji, S., Radhakrishnan, V.: Analysis of process parameters in surface grinding with graphite as lubricant based on the Taguchi method. *J. Mater. Process. Technol.* **141**(1), 51–59 (2003). doi:[10.1016/s0924-0136\(02\)01112-3](https://doi.org/10.1016/s0924-0136(02)01112-3)
23. Taguchi, G.: *Introduction to Quality Engineering*. Asian Productivity Organization (APO) (1990)
24. Nalbant, M., Gokkaya, H., Sur, G.: Application of Taguchi method in the optimization of cutting parameters for surface roughness in turning. *Mater. Des.* **28**(4), 1379–1385 (2007). doi:[10.1016/j.matdes.2006.01.008](https://doi.org/10.1016/j.matdes.2006.01.008)
25. Parton, H., Baets, J., Lipnik, P., Goderis, B., Devaux, J., Verpoest, I.: Properties of poly(butylene terephthalate) polymerized from cyclic oligomers and its composites. *Polymer* **46**(23), 9871–9880 (2005). doi:[10.1016/j.polymer.2005.07.082](https://doi.org/10.1016/j.polymer.2005.07.082)
26. Ross, P.J.: *Taguchi Technique for Quality Engineering*. McGraw-Hill (1998)
27. Roy, R.K.: *A Primer on Taguchi Method*. Van Nostrand Reinhold (1990)